Towards a millivolt optical modulator with nano-slot waveguides

M. Hochberg[1], T. Baehr-Jones[1], G. Wang[1], and J. Huang[1], P. Sullivan[2] and L. Dalton[2], and A. Scherer[3]

[1]*Department of Applied Physics, California Institute of Technology, 1200 E California Blvd., Pasadena CA 91125*
[2]*Department of Chemistry, University of Washington, 109 Bagley Hall Box 351700, Seattle WA 98195*
[3]*Department of Applied Physics, California Institute of Technology, 1200 E California Blvd., Pasadena CA 91125*
tbaehrjones@yahoo.com, michael.hochberg@yahoo.com
psull76@u.washington.edu, dalton@chem.washington.edu
etcher@caltech.edu

Abstract: We describe a class of modulator design involving slot waveguides and electro-optic polymer claddings. Such geometries enable massive enhancement of index tuning when compared to more conventional geometries. We present a semi-analytic method of predicting the index tuning achievable for a given geometry and electro-optic material. Based on these studies, as well as previous experimental results, we show designs for slot waveguide modulators that, when realized in a Mach-Zehnder configuration, will allow for modulation voltages that are orders of magnitude lower than the state of the art. We also discuss experimental results for nano-slot waveguides.

OCIS Codes: (040.0040) Detectors; (040.6040) Silicon; (060.4080) Modulation; (130.0130) Integrated Optics; (130.2790) Guided Waves; (130.3120) Integrated Optics Devices; (160.5470) Polymers; (230.0040) Detectors

References and links

1. N. Bloembergen, P. S. Pershan and L. R. Wilcox, "Microwave modulation of light in paramagnetic crystals," Phys. Rev. **120**, 2014-2023 (1960).
2. Y. Yamabayashi and M. Nakazawa, "Terabit transmission technology," NTT. Rev. **11**, 23-32 (1999).
3. Y. Q. Shi, C. Zhang, H. Zhang, J. H. Bechtel, L. R. Dalton, B. H. Robinson and W. H. Steier, "Low (sub-1-volt) halfwave voltage polymeric electro-optic modulators achieved by controlling chromophore shape," Science **288**, 119-122 (2000).
4. O. Mitomi, K. Noguchi and H. Miyazawa, "Broadband and low driving-voltage LiNbO3 optical modulators," IEEE Proc. Optoelectron. **135**, 360-364 (1998).
5. D. Rutledge, "Filters," in *The Electronics of Radio* (Cambridge University Press, Cambridge, 1999).
6. M. M. de Lima, M. Beck, R. Hey and P. V. Santos, "Compact Mach-Zehnder acousto-optic modulator," Appl. Phys. Lett. **89**, 3 (2006).
7. E. L. Wooten, K. M. Kissa, A. Yi-Yan, E. J. Murphy, D. A. Lafaw, P. F. Hallameier, D. Maack, D. V. Attanasio, D. J. Fritz, G. J. McBrien, D. E. Bossi, "A review of lithium niobate modulators for fiber-optic communications systems," IEEE J. Sel. Top. Quantum Electron. **6**, 69-82 (2000).
8. M. Lipson, "Guiding, modulating, and emitting light on silicon - Challenges and opportunities," J. Lightwave Technol. **23**, 4222-4238 (2005).
9. H. Fukano, T. Yamanaka, M. Tamura and Y. Kondo, "Very-low-driving-voltage electroabsorption modulators operating at 40 Gb/s," J. Lightwave Technol. **24**, 2219-2224 (2006).
10. M. T. Tinker and J. B. Lee, "Thermal and optical simulation of a photonic crystal light modulator based on the thermo-optic shift of the cut-off frequency," Opt. Express **13**, 7174-7188 (2005).
11. Y. Enami, C. T. Derose, D. Mathine, C. Loychik, C. Greenlee, R. A. Norwood, R. D. Kim, J. Luo, Y. Tian, A. K. Y. Jen and N. Peyghambarian, "Hybrid polymer/sol–gel waveguide modulators with exceptionally large electro–optic coefficients," Nature Photon. **6**, 180-185 (2007).
12. A. S. Liu, R. Jones, L. Liao, D. Samara-Rubio, D. Rubin, O. Cohen, R. Nicolaescu and M. Paniccia, "A high-speed silicon optical modulator based on a metal-oxide-semiconductor capacitor," Nature **427**, 615-618 (2004).
13. J. J. Whelehan, "Low-noise amplifiers- then and now," IEEE Trans. on Microwave Theory Techniques **50**, 806-813 (2002).
14. H. Tazawa, Y. Kuo, I. Dunayevskiy, J. Luo, A. K. Y. Jen, H. Fetterman and W. Steier, "Ring resonator based electrooptic polymer traveling-wave modulator," IEEE J. Lightwave Technol. **24**, 3514-3519 (2006).

#81417 - $15.00 USD Received 23 Mar 2007; revised 9 Jun 2007; accepted 14 Jun 2007; published 20 Jun 2007

15. V. R. Almeida, Q. F. Xu, C. A. Barrios and M. Lipson, "Guiding and confining light in void nanostructure," Opt. Letters **29**, 1209-1211 (2004).
16. T. Baehr-Jones, M. Hochberg, G. X. Wang, R. Lawson, Y. Liao, P. A. Sullivan, L. Dalton, A. K. Y. Jen, A. Scherer, "Optical modulation and detection in slotted Silicon waveguides," Opt. Express **13**, 5216-5226 (2005).
17. Professor Larry R. Dalton, Chemistry Department, University of Washington, Box 351700, Seattle, WA, 98195 (personal communication 2006).
18. T. Baehr-Jones, M. Hochberg, C. Walker and A. Scherer, "High-Q ring resonators in thin silicon-on-insulator," Appl. Phys. Lett. **85**, 3346-3347 (2004).
19. A. Yariv, "The Modulation of Optical Radiation," in *Quantum Electronics* (John Wiley and Sons, New York, 1989).
20. T. Baehr-Jones, M. Hochberg, C. Walker, E. Chan, D. Koshinz, W. Krug and A. Scherer, "Analysis of the tuning sensitivity of silicon-on-insulator optical ring resonators," IEEE J. Lightwave Technol. **23**, 4215-4221 (2005).
21. M. Hochberg, T. Baehr-Jones, C. Walker, J. Witzens, L. C. Gunn and A. Scherer, "Segmented waveguides in thin silicon-on-insulator," J. Opt. Soc. Am. B **22**, 1493-1497 (2005).
22. G. Wang, M. Hochberg, and T. Baehr-Jones are preparing a manuscript to be called "Design and Fabrication of Segmented, Slotted Waveguides for Electro-Optic Modulation."
23. T. Baehr-Jones, M. Hochberg, C. Walker, and A. Scherer, "High-Q optical resonators in silicon-on-insulator-based slot waveguides," Appl. Phys. Lett. **86**, 81101-81104 (2005).

1. Introduction

Optical modulators are fundamental components of optical data transmission systems, serving as the gateway from the electrical to the optical domain [1]. High-bandwidth optical signals can be transmitted through optical fibers with low loss and low latency [2] making optical data transmission an attractive option for many applications. All practical high-speed modulators that are in use today require input voltage shifts on the order of 1V to obtain full extinction [3], however it is extremely advantageous in terms of noise performance for modulators to operate at lower drive voltages [4]. Many sensors and antennas generate millivolts or less [5]; as a result it is often necessary to include an amplifier in optical transmission systems, which often limits system performance.

A variety of physical effects are available to produce optical modulation, including the acousto-optic effect [6] and the Pockels' effect, which can be found in materials such as lithium niobate [7] or in poled electro-optic polymers. Other relevant effects include free-carrier plasma-dispersion [8], electro-absorption [9], and thermal modulation [10]. For most types of practical optical modulator, the basic designs are similar; a region of waveguide on one or both arms of a Mach-Zehnder interferometer is made to include an optical material that changes its refractive index in response to an external electrical signal. In the case of Pockels' effect devices, voltage is generally introduced to the waveguide region by means of external electrodes. This causes the active region to shift in index slightly, causing a phase delay for photons traveling down one arm of the modulator. When the light in that arm is recombined with light that traveled down a reference arm, the phase difference between the two signals causes the combined signal to change in amplitude. Figure 1 panel A shows a diagram of a conventional Pockels' Effect modulator.

#81417 - $15.00 USD Received 23 Mar 2007; revised 9 Jun 2007; accepted 14 Jun 2007; published 20 Jun 2007

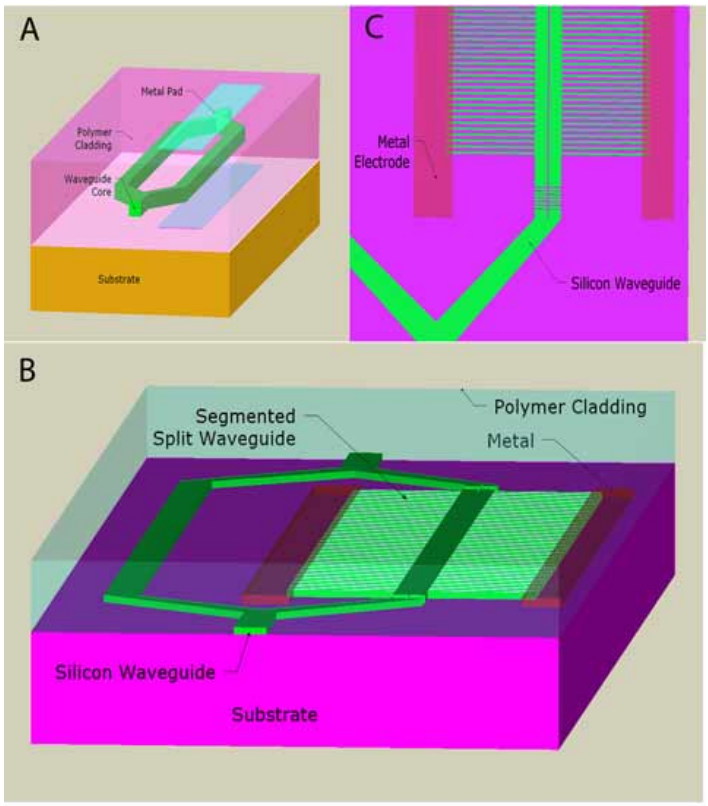

Fig. 1. Panel A: Isometric three dimensional schematic of a conventional Mach-Zehnder polymer interferometer, showing top contact, waveguide, and bottom contact layers. Panel B: Top-down layout of a slot-waveguide based optical modulator. C: Three dimensional, isometric schematic of a slot-waveguide modulator, showing the slot waveguide, segmentation region and metal contacts. The device functions by maintaining the two arms of the slot waveguide at differing voltages, creating a strong electric field in the slot.

The measure of the strength of a modulation effect is the refractive index shift obtained for a given input voltage. Today's best modulators obtain effective index shifts on the scale of 10^{-5} for 1 V [3, 11]. This implies that a Mach-Zehnder 1 cm in length, meant to modulate radiation near 1550 nm, would require a halfwave voltage around 2 V. The halfwave voltage, $V\pi$, is the external input needed for the arms to accumulate a relative phase shift of π. Usually the length-independent product V_π-L is reported; typical V_π-L values are in the range of 8 V-cm in Silicon [12], or 6 V-cm for lithium niobate modulators [4]. This voltage-length product is the best figure of merit for examining a novel modulator design; making a modulator physically longer generally trades lower halfwave voltage against reduced operating frequency and higher loss. Because generating both high-speed and high-power signals requires specialized amplifiers [13], lowering the operating voltage of modulators is extremely desirable, particularly for on-chip integrated electronic/photonic applications (including chip-to-chip interconnects) where operating voltages are limited.

In the case of electro-optic modulation, the actual shift in index of the active material is not proportional to the applied voltage; it is proportional to the electric field induced by this voltage. Therefore, simply moving the drive electrodes closer together will have the effect of enhancing a V_π-L for a modulator. However, conventional polymer-based device geometries have typically involved metal or Indium-Tin-oxide electrodes, which must be isolated from

#81417 - $15.00 USD Received 23 Mar 2007; revised 9 Jun 2007; accepted 14 Jun 2007; published 20 Jun 2007

the optical mode field [14]. Our proposed class of modulator structures circumvents this limitation by utilizing the fact that a slot waveguide [15] is formed of two distinct silicon ridges. These ridges can be used as a pair of very closely spaced but electrically isolated electrodes. The divergence condition for a TE mode, moreover, causes the optical field to be concentrated in the region between the slots, located in precisely the same place as the field induced by a voltage difference between the two silicon arms.

Using a slot waveguide based electro-optic modulator geometry, we have previously demonstrated ring resonators with substantially better tunability (in Gigahertz per volt) than those built with comparable electrooptic materials in conventional geometries [16]. Here we present a detailed analysis of the manner in which the slot waveguide enhance the modulation effect, and we also present a study of a number of new designs. We find, very surprisingly, that making the slot smaller that the .14 μm geometry used previously increases the modulation effect, so that the modulation strength is nearly inversely proportional to the size of the gap. This is due to the fact that even for slots as small as .02 μm that the TE optical mode will still be largely concentrated in the central slot. This implies that nearly an additional order of magnitude in modulation enhancement can be obtained over the performance previously demonstrated. This, combined with recent developments of nonlinear polymers with r_{33} values of 130 pm/V [11] and 500 pm/V [17], suggests that it may soon be possible to build a modulator with a V_{π}-L on the order of 4 mV-cm, and resonators with tunability of .5 THz/V, substantial enhancements over the current state of the art.

2. Theoretical background

2.1 Waveguide susceptibility

The primary design goal of any electro-optic waveguide geometry is to maximize the amount of shift in effective index that will occur due to a given applied voltage. In order to predict this behavior, one must start with knowledge of the modal patterns associated with a given waveguide design. The exact modal patterns for the silicon slot waveguides under consideration can be calculated using a Hermetian eigensolver on the FDTD grid. Once the modal patterns are known from simulation, the shift in effective index due to an index shift in part of the waveguide can be readily calculated. The static electric field due to the two waveguide arms acting as electrodes can be calculated by solving the Poisson Eq.

The nonlinear polymers that have been used with slot waveguides exhibit a local anisotropic shift in their dielectric constant when they are exposed to an electric field. This is characterized by a value known as r_{33}, which is a component of the electro-optic tensor [19]. A simplification is appropriate to the case of slot waveguides, where the poling field, the modulation field, and the optical electric field are all nearly parallel. In this case, r_{33} is defined as:

$$\frac{1}{(n+\delta n)^2} - \frac{1}{n^2} = r_{33} E_{dc} \tag{1}$$

That is, a shift in the bulk index for this particular polarization is defined as a product of r_{33} and the modulating electric field. The local shift in relative dielectric constant for the optical frequency, for the TE mode, can then be expressed as:

$$\delta\varepsilon = -E_{dc}\left(n^4 r_{33}\right) \tag{2}$$

Here n is the bulk refractive index of the nonlinear polymer. We will drop the minus sign in what follows for convenience; the polarity of the r_{33} value can always be inverted in the poling process and is therefore arbitrary.

Take the x-y plane to be the plane of the waveguide, while the z direction is the direction of propagation. Imagine that the modulating electric field is non-negligible only in the x direction and uniform. In this case, using perturbation theory [20], the total shift in effective index for the optical mode can be calculated to be:

#81417 - $15.00 USD Received 23 Mar 2007; revised 9 Jun 2007; accepted 14 Jun 2007; published 20 Jun 2007

$$\delta n_{eff} = \frac{E_{dc}\int \left|\mathbf{E}_{opt}\cdot\mathbf{x}\right|^2 dA}{\int 2\,\mathrm{Re}\left(Ex_{opt}^{\ *}Hy_{opt} - Ey_{opt}^{\ *}Hx_{opt}\right)dA}\frac{1}{Z_0}\left(n^4 r_{33}\right) \tag{3}$$

The top integral is taken over only regions where the nonlinear polymer has been deposited and the modulating field is present, while the bottom integral should be taken over all space. The particular strength of the polymer, however, is not directly relevant to the waveguide geometry. It is convenient to factor the last term out of Eq. (3). Also, it is the ratio of the dc electric field to the applied voltage V that is most meaningful for a figure of merit. So, we define as the effective index susceptibility:

$$\gamma = \frac{(E_{dc}/V)\int \left|\mathbf{E}_{opt}\cdot\mathbf{x}\right|^2 dA}{\int 2\,\mathrm{Re}\left(Ex_{opt}^{\ *}Hy_{opt} - Ey_{opt}^{\ *}Hx_{opt}\right)dA}\frac{1}{Z_0} \tag{4}$$

The units of the effective index susceptibility are m^{-1}. The most useful parameter in characterizing a waveguide that is part of a modulator geometry is the derivative of the effective index with respect to applied voltage. It can be expressed in terms of our figure of merit as:

$$\frac{\partial n_{eff}}{\partial V} = \gamma\left(n^4 r_{33}\right) \tag{5}$$

This relationship expresses how much the effective index of the waveguide shifts in response to an applied voltage. Before continuing, it is useful to note an approximate maximum value for Eq. (4); in the case that the mode were contained entirely inside a material of a given index, we would have $n + \delta n = \sqrt{\varepsilon + \delta\varepsilon}$. It is in this situation that the mode is maximally sensitive to a shift in the waveguide index. Another simplification is possible if the modulating electric field is due to two parallel plates with gap distance g; then $E_{dc}/V = 1/g$. In this situation:

$$\gamma = 1/(2ng) \tag{6}$$

This provides a useful approximate upper bound on the effective index susceptibility that we can expect to obtain from any waveguide design. Conventional electrode designs where the optical mode is nearly entirely contained in the polymer often approach this value [14].

2.2 Projecting device performance

Before proceeding, we should consider how the performance of various active devices depends on the derivative of the effective index with respect to voltage. When one arm is positively biased and one arm negatively biased, a Mach-Zehnder modulator has a V_π-L given by:

$$V_\pi L = \frac{\pi}{2k_0(\partial n/\partial V)} \tag{7}$$

Here k_0 is the free space wavenumber of the optical signal under modulation. Ring resonators have also been used [15] to enable optical signals to be modulated or switched based on a nonlinear polymer being modulated by an external voltage. In this case, the performance of the tunable ring resonator is usually reported in the frequency shift of a resonance peak due to an externally applied voltage. This can be expressed as:

#81417 - $15.00 USD Received 23 Mar 2007; revised 9 Jun 2007; accepted 14 Jun 2007; published 20 Jun 2007

$$\frac{\partial f}{\partial V} = \frac{-\frac{c}{\lambda}\frac{\partial n}{\partial V}}{\left(n - \lambda \frac{\partial n}{\partial \lambda}\right)} \tag{8}$$

It is obvious that the tunability of a resonator and the value $1/(V_\pi\text{-}L)$ for a Mach-Zehnder modulator are both proportional to the figure of merit, γ. Thus, increasing the figure of merit will lead to better device performance for both ring and MZI geometries.

3. Device geometries

3.1 Previously realized geometries

It is useful to begin by noting the performance of a conventional polymer modulator device, which was realized by Tazawa et al [14]. By solving for the mode that the specified geometry would support, a γ of .026 μm^{-1} is obtained. This is close to a value that can be obtained by the approximate formula (6). Using the reported r_{33} value of 33 pm/V, one can then predict from (5) and (8) that about 1 GHz/V of tuning should be obtained, which was in fact observed. A diagram of the optical mode pattern and the modulating electric field for this geometry is shown in Fig. 3.

This can be compared to our previous results [18], where a γ of .4 μm^{-1} was obtained based on a slot of .14 μm. Because of this enhanced figure of merit compared to the conventional geometry, a tuning of 5.2 GHz/V was observed. This corresponds to an r_{33} of 22 pm/V (which was incorrectly reported in our previous paper as being approximately 50-100 pm/V due to a calculation error; the values reported for tunability, however, are correct. The authors regret the error). The benefit of the slot waveguide is apparent; for even a somewhat inferior modulation material, more tuning is obtained.

3.2 Proposed geometries

Motivated by the enhancement observed due to a slot size of .14 μm when compared to a conventional geometry, we performed a theoretical exploration of various slot waveguide designs. In particular, we were interested in seeing if further enhancement of tuning could be obtained on the basis of geometry. We explored narrowing the slot, making the slot arms taller, and even adding several slots. Our initial expectation was that the performance could not be increased much by narrowing the gap of the slot waveguide. Even though a given voltage would lead to a larger modulating field for the narrower gaps, we believed that the modal pattern would no longer have as good an overlap with the modulated material, and that there would turn out to be some optimum design which balanced the two effects.

Surprisingly, for the TE optical mode, this is not the case. For even very narrow gaps, on the order of 20-40 nm, the optical mode is still largely contained in the region between the two arms. This is due to the sharp discontinuity in the horizontal electric field due to the divergence free nature of the displacement electric field. As a result, the figure of merit, which is linearly proportional to the strength of the modulating field, increases in a fashion roughly inversely proportional to the gap size.

It is important to note a limitation in the analysis of these waveguides; because the modes cannot be solved analytically, the accuracy of the solution is limited by the discretization used in the numerical mode solver. We use a mode solver that has a uniform grid, with a minimum discretization of 5 nm used for the smallest slots. It is possible that there is some error in the solved mode pattern for the smallest slots that we have studied. However, as will be seen, there is a clear trend that starts with even larger slot waveguides, where the solved mode pattern is more accurate.

#81417 - $15.00 USD Received 23 Mar 2007; revised 9 Jun 2007; accepted 14 Jun 2007; published 20 Jun 2007

Table 1 shows the results of a design study involving a number of different slot waveguide configurations. We show what figures of merit will be for waveguides involving wider and narrower slots, higher arms, and those with more than one slot.

Waveguide Design	Waveguide Height (nm)	Arm Sizes (nm)	Maximum γ (μm^{-1})	Minimum γ (μm^{-1})
1	100	300, 300	1.3, 20nm gap	.40, 140nm gap
2	150	300, 300	1.6, 20nm gap	.68, 120nm gap
3	200	300, 300	2.3, 20nm gap	.74, 120nm gap
4	100	400, 400	1.1, 20nm gap	.67, 60nm gap, modal limit
5	100	250, 250	1.2, 20nm gap	.56, 60nm gap, modal limit
6	100	300, 40, 300	1.6, 20nm gap	.53, 80nm gap, modal limit
7	100	300, 40, 40, 300	1.9, 20nm gap	.76, 60nm gap, modal limit
8	200	200, 40, 200	3, 20nm gap	1.4, 60nm gap, modal limit
9	300	300, 300	2.5, 20nm gap	2.5, 20nm gap, modal limit
Tazawa et al	N/A	N/A	.026, 10 μm gap	N/A

Table 1: Predicted figures of merit for various proposed designs.

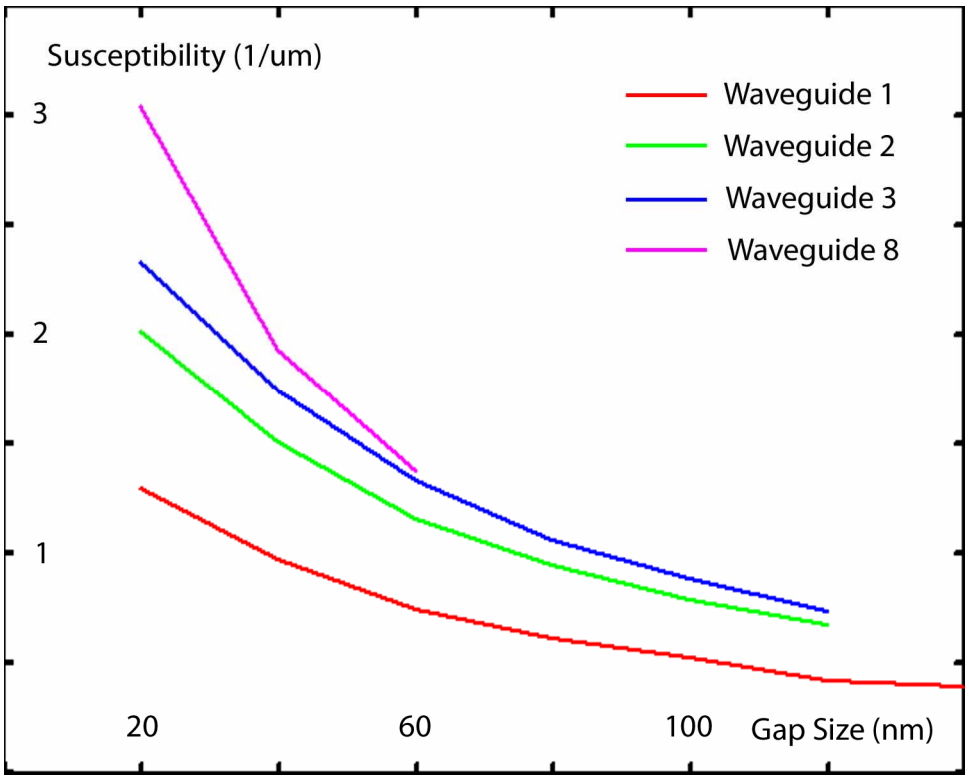

Fig. 2. A plot of various susceptibilities as shown in table 1 for differing gap sizes. Making the gap smaller leads to substantial improvements in the figure of merit.

#81417 - $15.00 USD Received 23 Mar 2007; revised 9 Jun 2007; accepted 14 Jun 2007; published 20 Jun 2007

One of the most optimal designs consists of a 200 nm thick SOI layer with arms 300 nm wide, and a single gap of 20 nm, as shown in Figs. 2 and 3. This design enjoys a figure of merit of γ=2.3 μm^{-1}; about two orders of magnitude better than the figure of merit for the conventional modulator design with external electrodes. If we combine this value with a nonlinear polymer of r_{33}=500 pm/V, we obtain $\partial n_{eff}/\partial V$=.01 V^{-1}. This level of tunability would lead to a Mach-Zehnder with a V_π-L of 4 mV-cm, and a resonator with tunability of .5 Thz/V. This design is shown in Fig. 3, along with the more conventional electrode geometry used by Tazawa et al [14].

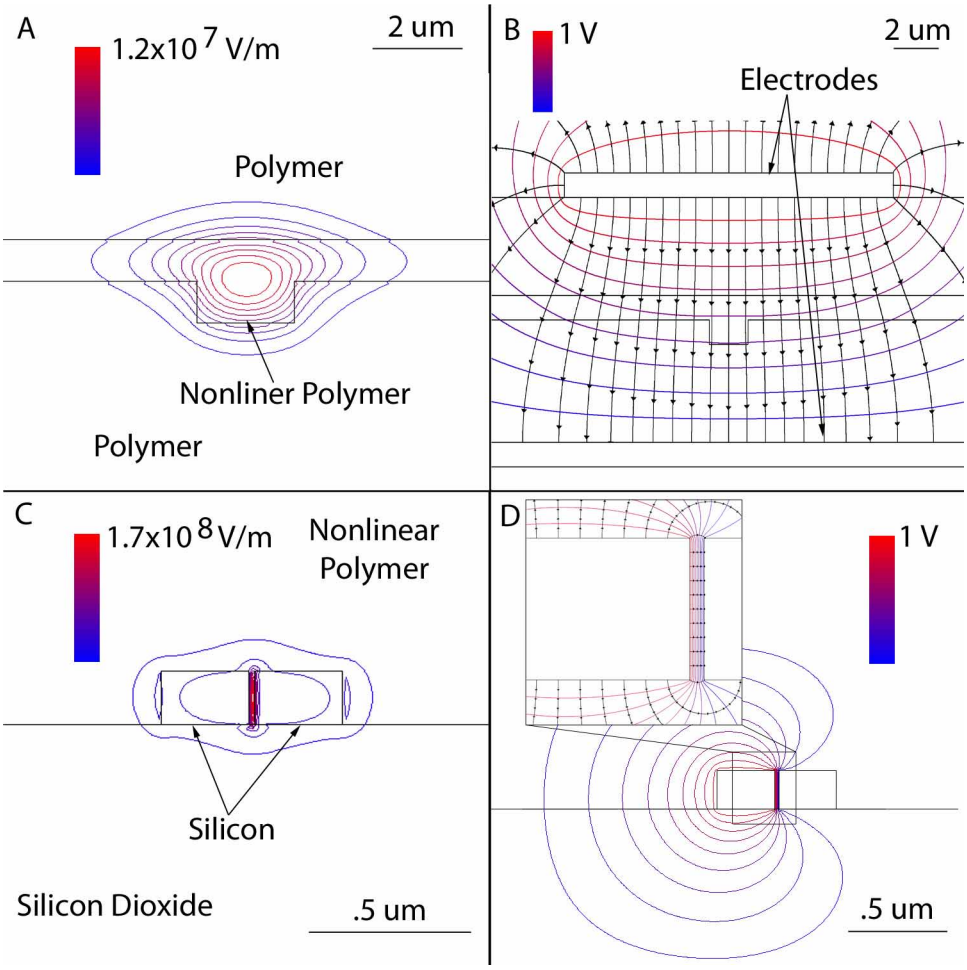

Fig. 3. Panels A and B show a conventional electrode geometry for a nonlinear polymer waveguide with the configuration used by Tazawa et al. Panel A shows the optical mode with |E| plotted in increments of 10%, for a mode with propagating power of 1 Watt. Panel B shows a contour plot of the static electric field, with the field of view slightly enlarged. Panels C and D show analogous data for the most optimal slot waveguide geometry. In the slot waveguide, the Silicon provides both the optical guiding layer and the electrical contacts.

One might doubt, incidentally, that a nonlinear polymer, however active, could change its effective index by as much as is implied by this figure. We stress that the actual driving voltage would probably be less than a volt in such an instance, and so the actual modulating electric field experienced by the polymer would not be much different from what is present in today's larger devices. The maximum drive voltage will be determined by the breakdown

#81417 - $15.00 USD Received 23 Mar 2007; revised 9 Jun 2007; accepted 14 Jun 2007; published 20 Jun 2007

field in the polymer, which is typically approximately 300 V/μm. This implies for a 20 nm gap a maximum drive voltage of 6 V.

We have recently demonstrated empirically that slot sizes of around 70 nm can be fabricated in 110 nm SOI as ring resonators with electrical contacts, as shown in Fig. 4. These waveguides would have figures of merit about a factor of 2 higher than we have previously achieved with 140 nm slots. A Q of around 8k has been obtained, which, when combined with the massive amounts of tuning we expect, should prove sufficient for many applications. The Q does not approach the value we have obtained with non-electroded slotted ring resonators due to excess loss from the electrical contacts. The same electrode geometry was used as in our previous result [16]. We have also confirmed through electrical measurements that the two halves of the slots are largely electrically isolated. For further information concerning the coupler apparatus used and the specifics of a slot ring resonator, the reader is referred to [23]. Work is currently underway to fabricate and characterize the optical performance of slot ring resonators with slot widths at and below 40 nm.

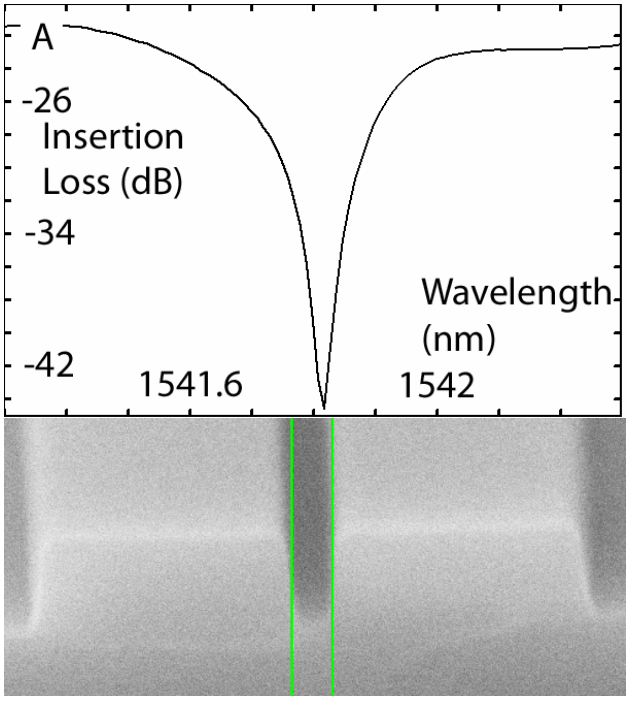

Fig. 4. Panel A shows a transmission spectra of an electroded slot waveguide resonator with a gap of 70 nm. Fiber to fiber insertion loss is plotted in dB, against the test laser wavelength in nm. Panel B shows an SEM image of a portion of a typical slot waveguide with a sub-100 nm slot. The cursor width is 57 nm in this image.

Lastly, we would note the possibility of constructing even narrower slot waveguides, on the scale of 1-5 nm in thickness, by using epitaxial techniques to grow a horizontal slot structure with an active, insulating material, with silicon beneath and above. Such structures offer the possibility of yet another order of magnitude of improvement in the low-voltage performance of modulators. Here we should also mention that we anticipate our slot structures to be fairly robust even in the presence of fabrication errors. Fabrication imperfections may cause some of the narrower slots to have tiny amounts of residual silicon or oxide in their centers, or to even be partially fused in places. As long as electrical isolation is obtained, and the optical loss is acceptable, we would expect the slot performance to decrease only in a linear proportion to the amount of the slot volume that is no longer available to the nonlinear polymer cladding.

#81417 - $15.00 USD Received 23 Mar 2007; revised 9 Jun 2007; accepted 14 Jun 2007; published 20 Jun 2007

3.3 Electrical considerations

As we have shown empirically, silicon can be doped to about 0.025 Ω-cm resistivity with an n-type dopant while only increasing losses approximately 5 dB/cm [16]. Other dopants or perhaps other high index waveguiding materials may have even higher conductivities that can be induced, without significantly degrading optical performance. However, it is known that the conductivity cannot be increased endlessly without producing substantial optical loss.

This naturally presents a serious challenge for the issue of driving a slot waveguide of any substantial length. Consider a slot waveguide arm of length 1 mm, formed of our optimal design. The capacitor formed by the gap between the two electrodes is about .25 pF. The 'down the arm' resistance of the structure, however, is 4 MΩ. Therefore, the turn-on time of an active waveguide based on this is about .1 μS, implying a 10 MHz bandwidth. Analogous limitations will be encountered in tunable ring resonators.

A solution to this problem is presented by contacting the waveguide via half-etched, continuous contacts on either side of the waveguide or by using a segmented waveguide. While the former has the advantage of theoretical simplicity and potentially better performance, it would require several different high resolution lithography steps in a single process. The segmented approach consists of contacting the two silicon ridges with a series of silicon arms, and can be done with a single lithographic step. Even though the silicon arms destroy the continuous symmetry of the waveguide, for the proper choice of periodicity minimal excess loss occurs, and the mode is not substantially distorted, as can be shown via simulation. We have previously demonstrated empirically that electrical contact can be formed for non-slotted waveguide via segmentation with relatively low optical losses [21]. We have very recently demonstrated the same thing with slotted waveguides; with the choice of a proper periodicity, both sides of the slotted waveguide can be contacted quasi-continuously in a single lithographic layer to a metal lead, leading to intrinsic RC turn-on times in the hundreds of gigahertz. We have built and tested such structures, and found them to have low losses, and will describe the results in detail in a forthcoming article [22].

4. Conclusions

We have presented a series of slot waveguide designs that have been chosen to allow modulation based on an electro-optic polymer cladding. Some of our less optimal, previously published, designs have already been realized and showed nearly an order of magnitude improvement in resonance tunability when compared to conventional electrode geometries. Our best predicted designs show a further order of magnitude enhancement. This is a surprising outcome, since it it not intuitive that making slots narrower would provide better modulation performance even as the slots become far-subwavelength. However, the continuity conditions on the fields dictate that a substantial fraction of the field remains even in these nanoscale slots, making them ideal for constructing ultra-low V_π electrooptic modulators. We also note that that our designs do not require a nonlinear polymer per se – any electro-optic material that can be conformally coated or otherwise placed in a slot as shown in this paper would work. The only requirements are that the index of the material must be low, and the electrical resistance must be high.

When combined with the large electro-optic coefficients that have recently been realized with nonlinear polymers, our results suggest that millivolt-cm scale V_π-L modulators are now possible.

Acknowledgments

This work was supported in part by the Air Force Office of Scientific Research and the Cornell Nanoscale Facility, which is funded as part of the National Nanotechnology Infrastructure Network by the National Science Foundation.

#81417 - $15.00 USD Received 23 Mar 2007; revised 9 Jun 2007; accepted 14 Jun 2007; published 20 Jun 2007